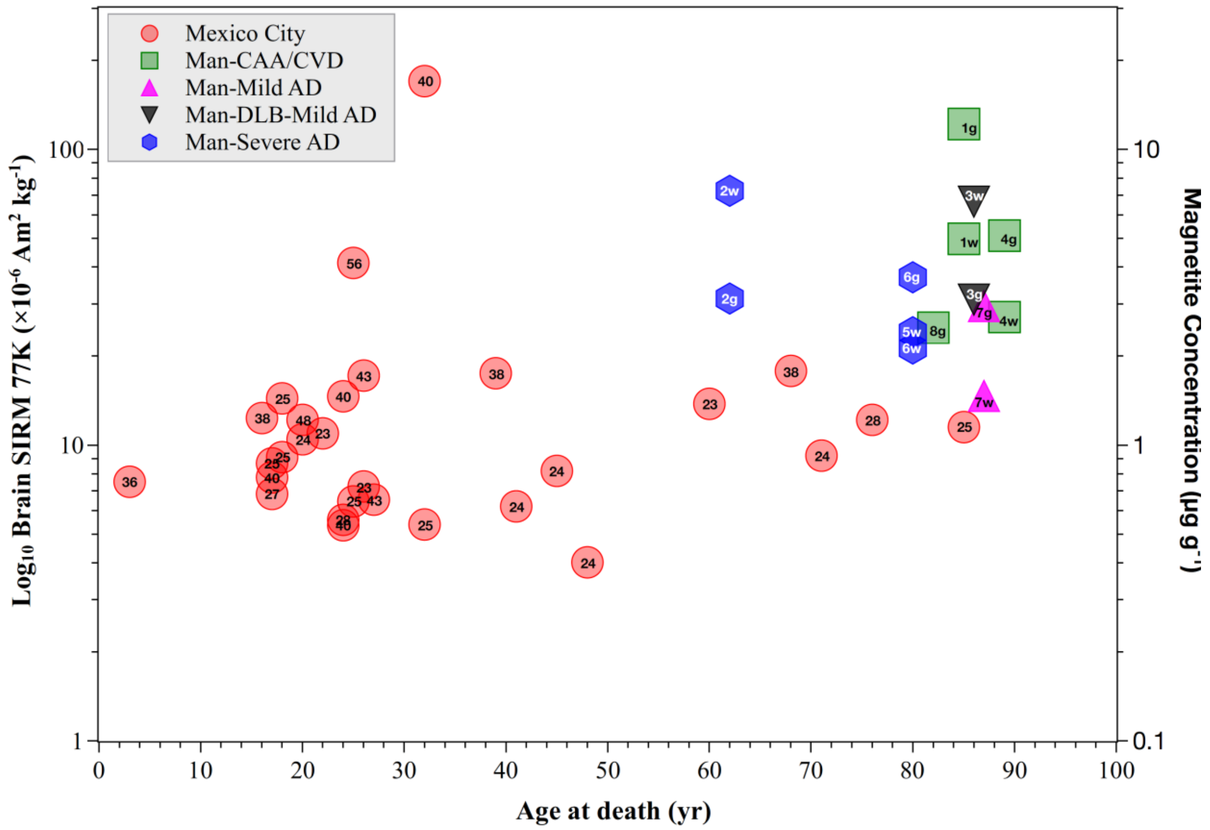

Fig. S1 SIRM 77 K (10^{-6} Am^2 kg^{-1}) and estimated magnetite concentration (μg g^{-1}) for frontal cortex samples versus age at death, Mexico City and Manchester cases. The annual mean airborne $PM_{2.5}$ concentration (μg m^{-3}) is given for the residence area of the Mexican cases (inside each data symbol); SIRM values for gray (g) and white (w) matter are given for the Manchester cases, together with their clinical diagnosis upon death (CAA = cerebral amyloid angiopathy; CVD = cerebrovascular disease; DLB = dementia with Lewy bodies, see Table 1).

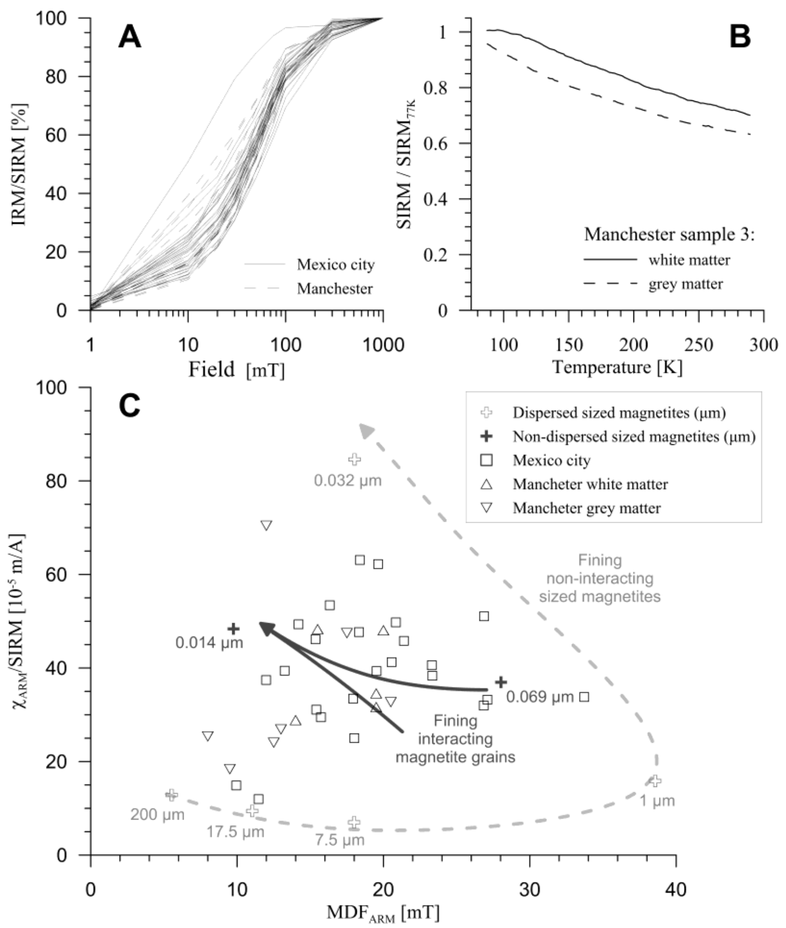

Fig. S2: Magnetic analyses of brain tissue samples (freeze-dried): A) acquisition of isothermal (RT) remanent magnetization in applied direct current (DC) fields from 5 mT to 1 T. All samples acquire most of their magnetization at fields < 100 mT, indicating the dominant presence of ferrimagnetic minerals (e.g. magnetite and/or maghemite). The magnetically-softest sample (the Mexico City case to the left of all remaining samples) has the highest SIRM value (case 282). B) Measurement of LT remanence (77 K, dc field 1 T) upon warming to RT, showing the thermal unblocking of the superparmagnetic particles. C) Comparison between the brain samples and sized, synthetic magnetites of known grain size and degree of dispersion[30], as measured by the RT anhysteretic remanent magnetization (ARM), normalized by the SIRM, plotted against the median destructive field of the ARM (MDF_{ARM}, in mT). All of the measurable brain samples fall within the region of the least-dispersed synthetic, sub-micrometre magnetites, indicating magnetic interactions, and hence agglomeration/clustering of some of the brain magnetite particles.

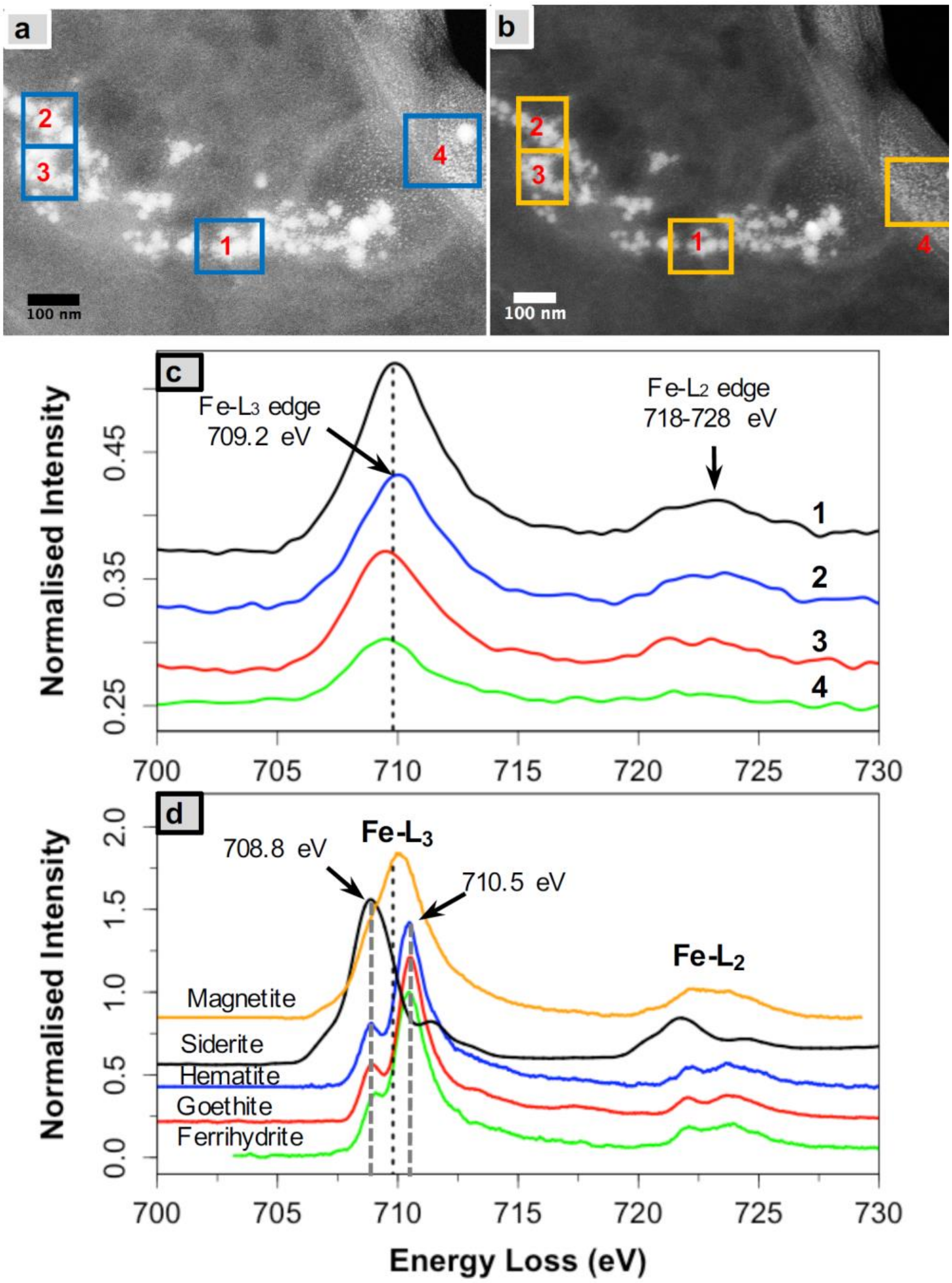

Fig. S3: High-angle annular diffraction (HAADF) (a) and dark-field (b) TEM micrographs showing spherical magnetic nanoparticles in brain tissues. (c) Fe-$L_{2,3}$ EELS spectra of nanoparticles identified in the selected areas (boxes: 1-4) showing the absence of any pre-edges (see hematite, goethite and ferrihydrite pre-edge at ~708.8 eV), Fe-L_3 edges centered at 708 eV and broad Fe-L_2 features characteristic of magnetite, compared with the Fe-L_{23} EELS spectra in (d) of standard magnetite, siderite, hematite, goethite and 2-line-ferrihydrite.

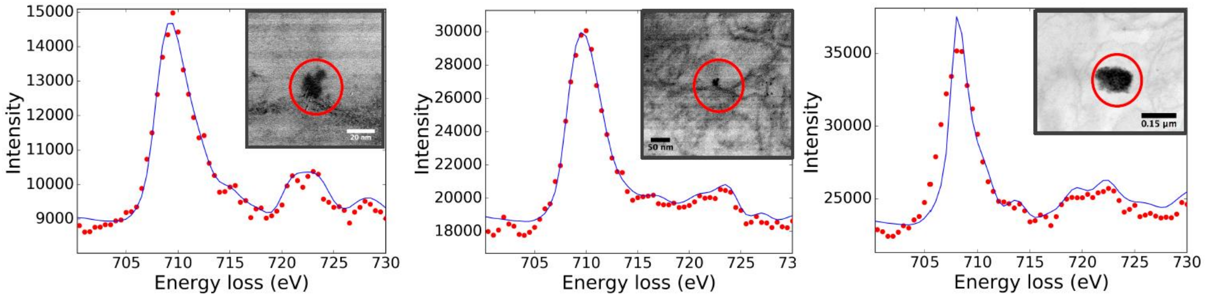

Fig. S4: Fe-$L_{2,3}$-edge spectra of magnetic particles found in brain samples. The Fe-L_3 and Fe-L_2 edges in all three samples are at 708.7-709.8 and 72-723 eV, in excellent agreement with the chemical shift in EELS spectra for the magnetite structure (also see Fig. S3).

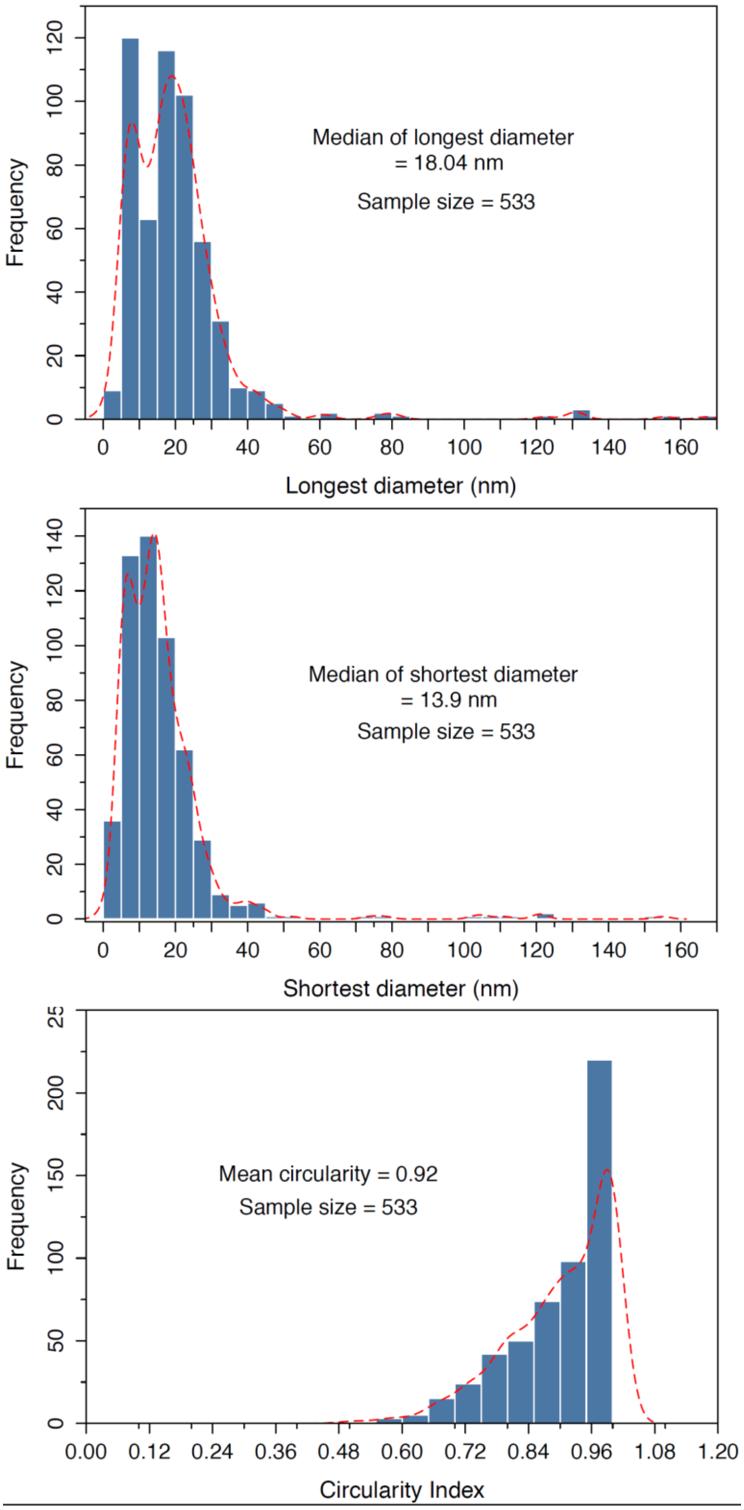

Fig. S5: Particle size distribution of magnetic particles in brain magnetic extracts. Particle size measurements were carried out on all the HRTEM micrographs collected from 6 brain magnetic extracts from different subjects. The ImageJ software package was used to describe the imaged particles (spherical and non-spherical) in terms of the longest and shortest diameters, perimeter projected area, or equivalent spherical diameter.

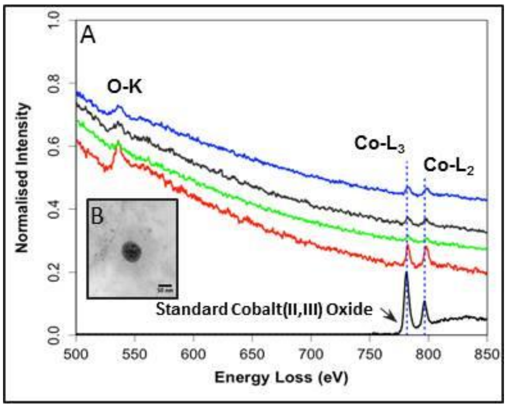

Fig. S6: Co-$L_{2,3}$ EELS spectra of cobalt (II,III) oxide nanoparticles associated with magnetite particles in brain tissues. Co-L_3 and Co-L_2 edges from different areas of a brain tissue sample (a) are centred at ~780 and ~796 eV, respectively, in a good match with an EELS spectrum of a standard cobalt (II,III) oxide.

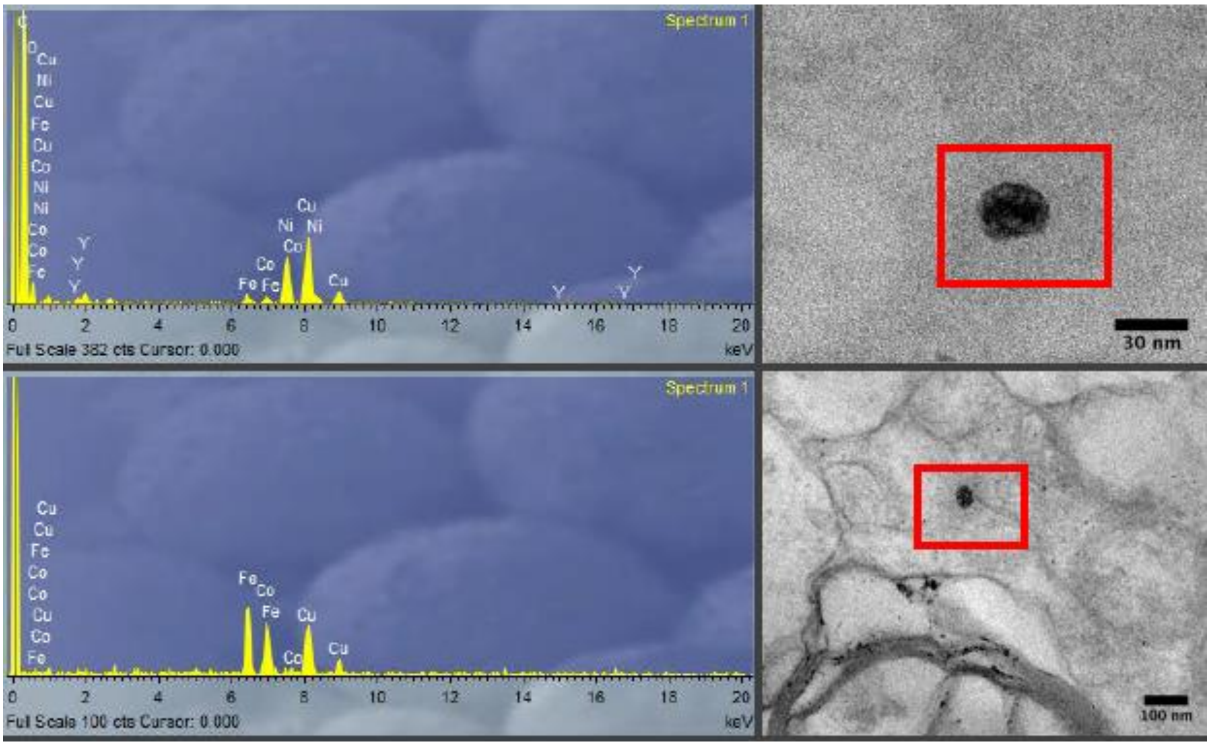

Fig. S7: Energy dispersive X ray analysis of metal-bearing NPs in brain tissue samples, showing presence of Fe, Ni, Co (and possibly Cu, with the caveat that the samples were mounted on holey carbon films on Cu grids).

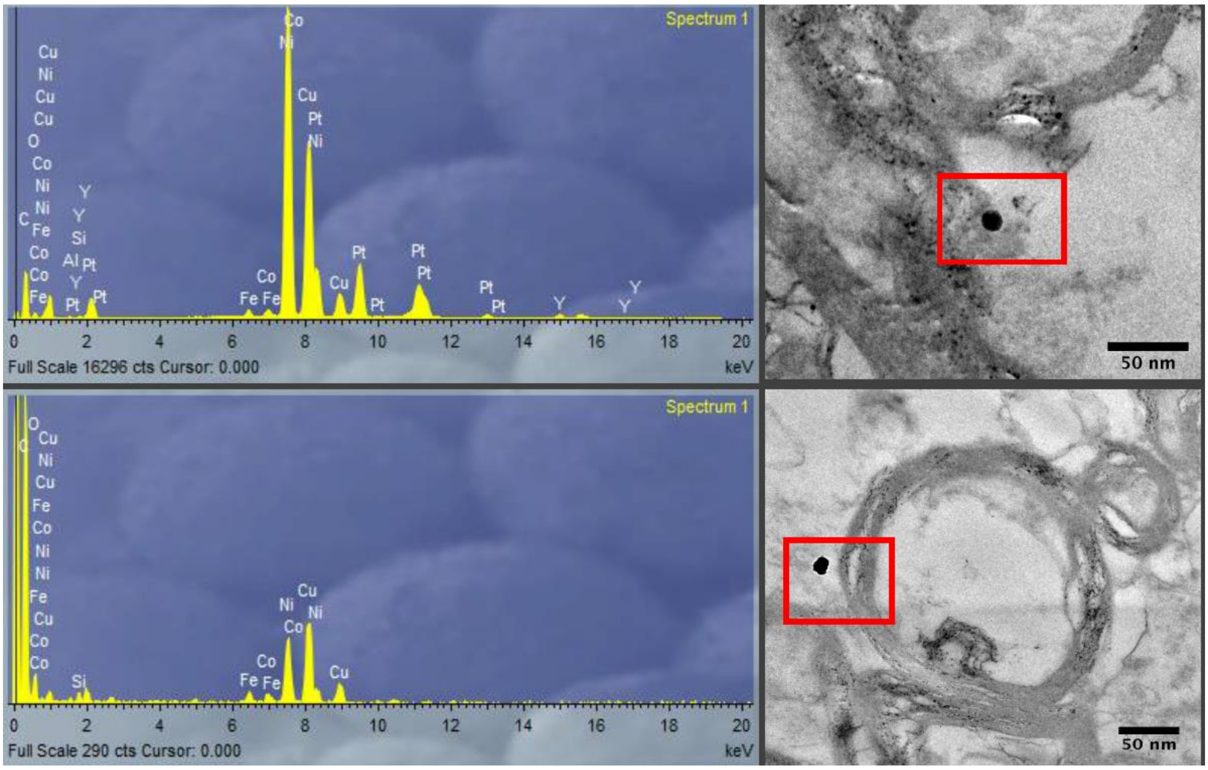

Fig. S8: Energy dispersive X ray analysis of metal-bearing NPs in brain tissue samples, showing the presence of Fe, Ni, Pt, Co and possibly Cu.

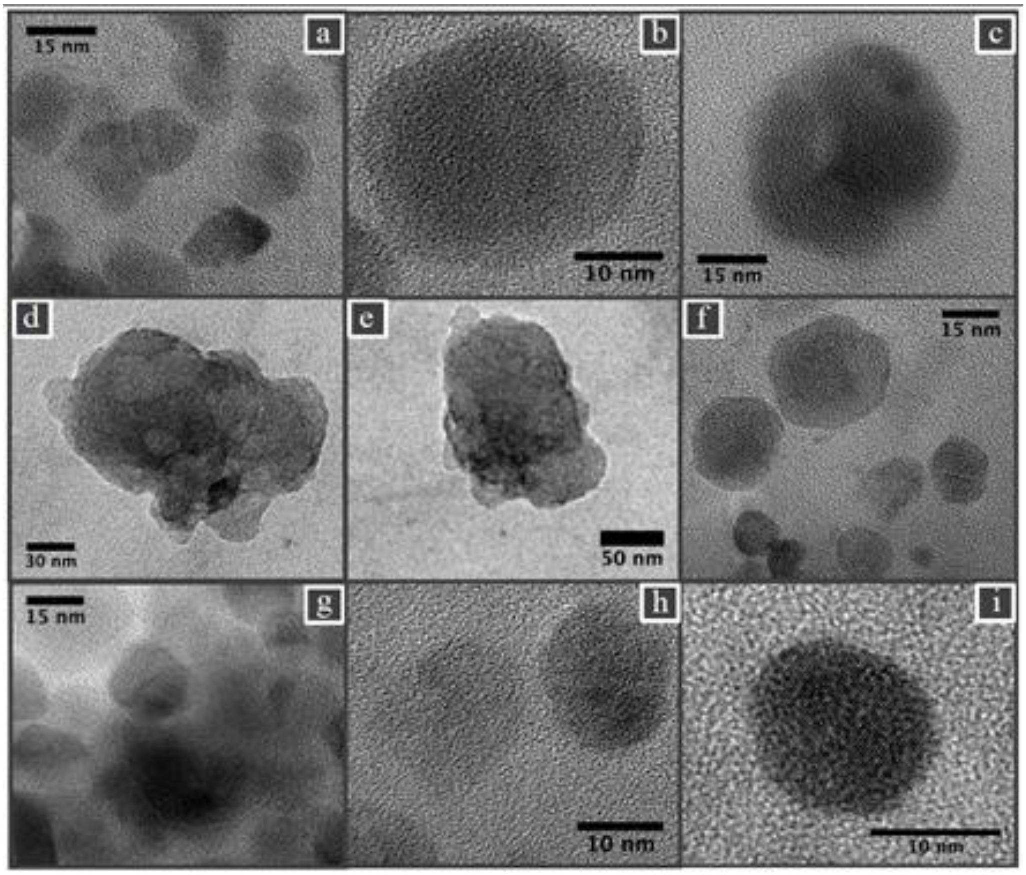

Fig. S9: A collection of HRTEM micrographs of magnetite particles, extracted from brain tissues, showing dominant rounded morphologies. Micrograph (c) shows fused magnetite particles and micrographs (d) and (e) show aggregated magnetite particles.

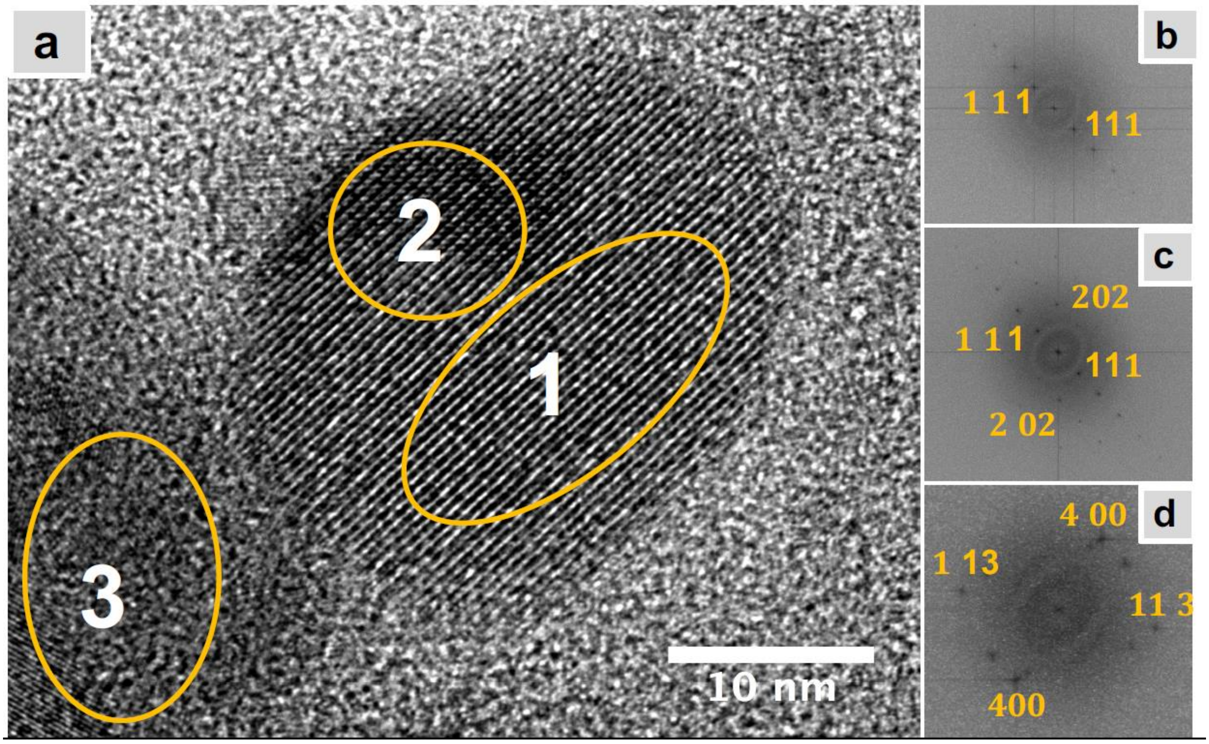

Fig. S10: HRTEM micrograph of magnetically-extracted magnetite particles from brain tissues. (b-d) FFT patterns of selected areas (1-3, respectively) featuring a single crystal in (b) and magnetite particles superimposed at ~90° in (c) and (d).

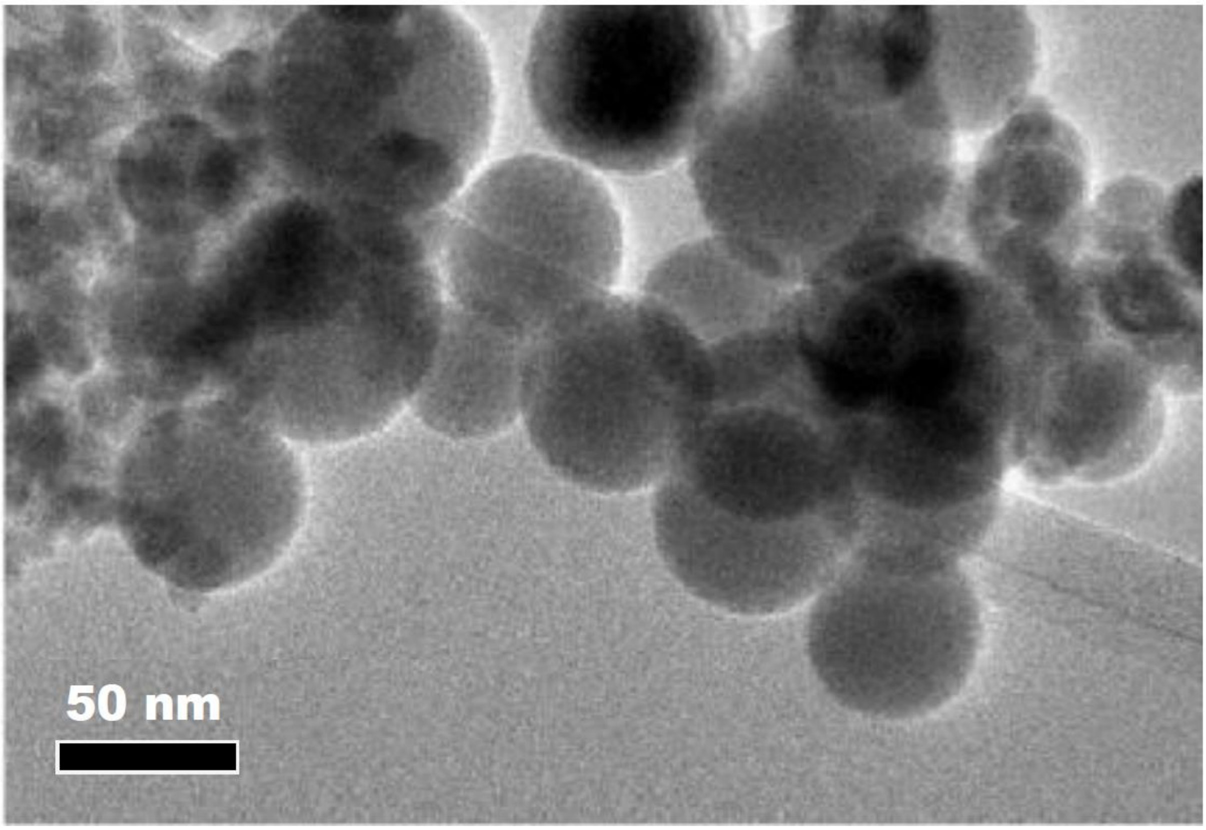

Fig. S11: TEM image of magnetite nanoparticles captured from the exhaust plume of a diesel engine (adapted from Liati et al., 2015).